Pergamon

Geochimica et Cosmochimica Acta, Vol. 66, No. 2, pp. 257–272, 2002

0016-7037/02 $22.00 + .00

PII S0016-7037(01)00779-7

Advection and removal of ^{210}Pb and stable Pb isotopes in the oceans: A general circulation model study

GIDEON M. HENDERSON[1,*] and ERNST MAIER-REIMER[2]

[1]Department of Earth Sciences, University of Oxford, Parks Road, Oxford OX1 3PR, United Kingdom [2]Max-Planck-Institut fur Meteorologie, Bundesstrasse 55, 20146 Hamburg, Germany

(*Received September* 25, 2000; *accepted in revised form July* 24, 2001)

Abstract—Natural Pb-isotope variability in the oceans encodes information about the sources of continental material to the oceans, about ocean circulation, and about Pb removal. In order to use this information, we must understand the natural cycle of Pb in the oceans, which is overprinted by large anthropogenic input. In this study we use ^{210}Pb, which has not been significantly anthropogenically perturbed, to investigate oceanic Pb. GEOSECS ^{226}Ra and model-derived atmospheric fluxes of ^{210}Pb are used to input ^{210}Pb into an ocean general circulation model. Irreversible scavenging of this ^{210}Pb onto settling biogenic particles and at the seafloor are tuned so that the model replicates the observed pattern of ^{210}Pb in the oceans. The best-fit model run provides a map of the variability of residence time for Pb. The global average residence time of Pb in this model is 48 yr, but there is over an order of magnitude variation between areas of high and low productivity. This is expected to enhance provinciality of Pb isotope ratios in the oceans. Because stable Pb isotopes are expected to behave in seawater in a similar fashion to ^{210}Pb, the pattern of removal of ^{210}Pb derived by the model can be used to investigate the behavior of stable Pb isotopes. We use a simplified input of Pb consisting of five point sources representing major rivers and a disseminated dust input. Although this simplified input scheme does not allow precise reconstruction of Pb concentration and isotopes in the oceans, it allows us to answer some first-order questions about the behavior of Pb as an ocean tracer. With a total Pb input of 6.3×10^7 mol/yr (Chow T. J. and Patterson C. C., "The occurrence and significance of Pb isotopes in pelagic sediments," *Geochim. Cosmochim. Acta* **26,** 263–308, 1962), the model predicts natural seawater Pb concentrations averaging 2.2 pmol/kg. Even in the absence of anthropogenic input, the model ocean exhibits a near-surface maximum in Pb concentration. And the model suggests natural Pb concentrations in the Northern Hemisphere an order of magnitude higher than in the Southern Hemisphere. A point source of Pb is suggested to dominate the seawater Pb inventory close to the source but is reduced to typically less than 10% of the inventory by the time that Pb is advected out of the originating ocean. This length scale of advection for Pb isotope signals confirms their potential as tracers of ocean circulation. Assuming an 8% dissolution of dust, their input to the open ocean are seen to be a significant portion of Pb inventory throughout the oceans and make up >50% of the Pb inventory in the model's Southern Ocean. Finally, a preliminary investigation of the response of Pb-isotope distributions to changes in boundary conditions between glacial and interglacial times illustrates that significant variation in the Pb isotopes are expected in some regions, even for reasonably small changes in climate conditions.

1. INTRODUCTION

Pb-isotope ratios exhibit spatial variability in the oceans. This reflects differences in the isotope ratio of the sources of oceanic Pb and the short residence time of Pb in seawater (Abouchami and Goldstein, 1995; Chow and Patterson, 1959, 1962; von Blanckenburg et al., 1996). This spatial variability encodes information about the oceanic sources of Pb; about ocean circulation; and about the ultimate removal of Pb (e.g., Abouchami et al., 1997; Christensen et al., 1997; O'Nions et al., 1998). Pb isotopes could therefore provide information about the past distribution of continental weathering fluxes to the oceans. And Pb isotopes could provide information about past ocean circulation to complement that deduced from the nutrientlike tracers, Cd/Ca and δ^{13}C. These existing tracers are set in the surface ocean so that many sources of deep water are effectively labeled with the same Cd/Ca and δ^{13}C and cannot be distinguished. But different deep-water source areas generally have different Pb-isotope compositions, allowing discrimination of the sources.

To extract information from ocean Pb-isotope variability, we must deconvolve the effects of source, advection, and removal. This is made difficult by the dramatic increase of Pb in the oceans that has occurred in response to human activity. Previous attempts to understand the oceanic Pb cycle have followed several approaches. These include the use of two-dimensional models of Pb removal in ocean gyres to explain observed isotope values (Igel and von Blanckenburg 1999; von Blanckenburg et al., 1999) and the measurement of anthropogenic Pb to learn about the advection and removal of Pb (e.g., Sherrell and Boyle, 1992).

Another productive approach to the study of ocean Pb isotopes has been to use the radioactive Pb isotope, ^{210}Pb, to derive quantitative information about the removal of Pb from the oceans at single sites or in particular regions. The ^{210}Pb cycle is not thought to have been significantly perturbed by human activity, so observed distributions of ^{210}Pb can help us understand the advection and removal of Pb in the oceans (e.g., Cochran et al., 1990).

* Author to whom correspondence should be addressed (gideonh@earth.ox.ac.uk).

In this study, we collate existing data on the distribution and sources of ^{210}Pb to the oceans and use them to tune a fully three-dimensional global ocean model of Pb advection and removal. We use this model to investigate the mixing of stable Pb isotopes from various sources to answer question such as these: What is the distribution of Pb residence time in the oceans? How far from a point source of Pb is that source expected to control the seawater isotope composition? What is the ratio of aerosol to riverine derived Pb found in open-ocean waters? And what is the likely sensitivity of ocean Pb-isotope distributions to changing environmental conditions?

2. STABLE PB AND ^{210}PB CYCLES IN THE OCEANS

There are three possible sources of dissolved Pb to seawater: rivers, atmospheric dust dissolution, and mid-ocean–ridge interaction. Before anthropogenic perturbation, riverine inputs are expected to dominate the total dissolved Pb budget of the oceans.

On the basis of measurements of hydrothermal fluids, Chen et al. (1986) deduced that the total hydrothermal Pb input to the oceans is ≈2% of the total oceanic budget. A considerable portion of this 2% is expected to be rapidly removed by precipitation of sulfides and Mn-Fe particles, so hydrothermal Pb is not expected to be a major contributor to the dissolved oceanic Pb budget. This argument is, however, contradicted by evidence from some Pb-isotope studies of Mn crusts (Abouchami et al., 1997; Christensen et al., 1997), which show trends toward mid-ocean ridge Pb-isotope values. These trends may reflect the tendency of hydrothermal Pb to remain associated with Mn-Fe particles and therefore to be preferentially incorporated in Mn crusts. Or they may be biased by a few sites particularly influenced by hydrothermal activity. These isotope trends nevertheless indicate that some hydrothermal Pb enters seawater, but we consider this to be a minor part of the total oceanic budget.

The relative size of eolian vs. riverine sources is most easily assessed by consideration of the output of Pb from the ocean system. Chow and Patterson (1962) measured Pb isotopes and concentrations for ≈70 marine sediments from across the Atlantic and Pacific Oceans. They used leaching experiments and sediment mass balance to demonstrate that a significant portion of the Pb in marine sediments is authigenic and therefore derived from dissolved seawater Pb. They assessed the flux of such authigenic Pb to the sediment as 6.3×10^7 mol/yr. It is only possible to explain a small amount of such a flux of dissolved Pb by the dissolution of atmospheric dust, and the remainder must therefore enter the oceans in rivers. Constraints on the fraction of Pb entering the oceans from the atmosphere will be further discussed in section 5.1.

Human activity, particularly the addition of Pb to gasoline and the smelting of metal ores (Nriagu, 1979; Shen and Boyle, 1987), has dramatically increased the Pb flux to the oceans. Depending on location, atmospheric Pb fluxes have increased to between 5 and 10,000 times their natural levels (Patterson and Settle, 1987), and riverine fluxes have also increased dramatically. This perturbation is commonly thought to cause the observed near-surface maximum of Pb concentration in the oceans (Flegal et al., 1986; Shen and Boyle, 1988). This anthropogenic Pb makes the natural Pb system unobservable at present.

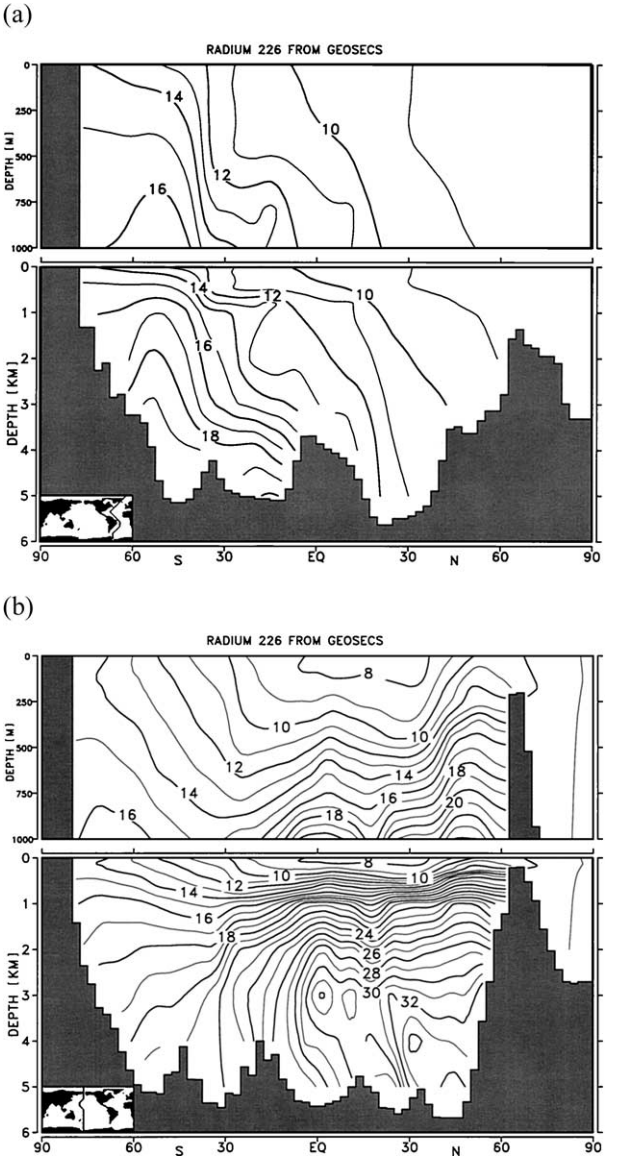

Fig. 1. Meridianal sections of ^{226}Ra concentrations for, a) the Atlantic and, b) the Pacific Oceans (see inset map for location). Units are dpm/100 L. Data are from GEOSECS and have been contoured with the flow fields of the Hamburg GCM.

^{210}Pb is a member of the ^{238}U decay series with a half-life of 22.3 yr. It is input to the oceans predominantly through the decay of ^{226}Ra in seawater. In addition, decay of ^{222}Rn in the atmosphere and subsequent rain-out provides an additional source of ^{210}Pb to the surface of the ocean. This additional source can lead to surface ^{210}Pb activities greater than those of ^{226}Ra. But in the deep ocean, the ^{210}Pb activities are lower than those of ^{226}Ra, reflecting the active removal of Pb from seawater on timescales comparable with the half-life of ^{210}Pb.

The flux of ^{222}Rn to the atmosphere may have been slightly perturbed by human activity through plowing and other soil disturbance. But these effects are small, and because the majority of oceanic ^{210}Pb comes from decay of ^{226}Ra, which is not

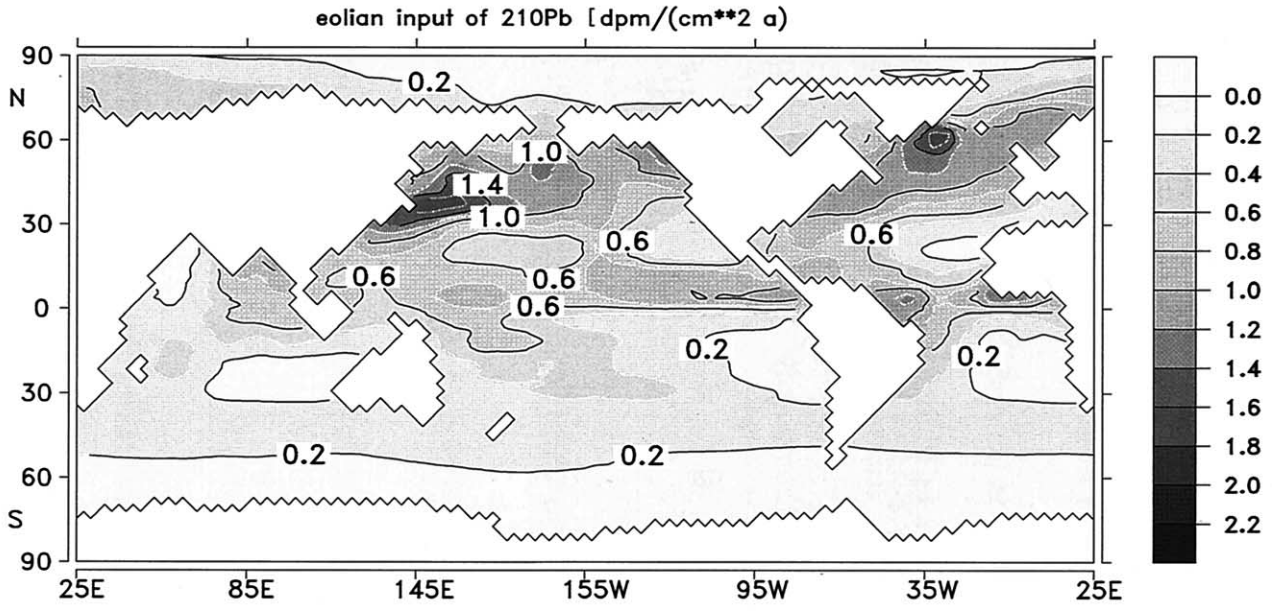

Fig. 2. Eolian input of ^{210}Pb to the surface ocean. Units are dpm/(cm^{2}a). Values were provided by Fritz Zaucker and are taken from an atmospheric model of ^{222}Rn sources and transport (Lin et al., 1996). The model values are in agreement with the sparse open-ocean measurements of eolian ^{210}Pb fluxes.

thought to be anthropogenically altered, the oceanic ^{210}Pb cycle is not expected to have altered significantly in response to anthropogenic change.

Although the sources of ^{210}Pb and stable Pb are very different from one another, their behavior within seawater and the mechanisms for their removal are expected to be identical. ^{210}Pb therefore offers the potential to accurately constrain the removal of stable Pb from the oceans and to help in deconvolving the importance of sources, advection, and removal on the Pb-isotope patterns observed in the present and past oceans.

3. MODEL OVERVIEW

The models used in this study are two well-documented ocean general circulation models developed by the Hamburg group. The first of these is the Hamburg large-scale geostrophic–ocean general circulation model (LSG-OGCM; Maier-Reimer et al., 1993), which derives ocean-circulation fields from basic fluid-dynamic principles. Derivation and performance of this model have been fully discussed elsewhere (Maier-Reimer et al., 1993; Winguth et al., 1999); this model provides velocity fields that correspond reasonably with those in the real world. For instance, the LSG-OGCM produces realistic salinity and density distributions in the oceans and creates ≈16 Sv of North Atlantic Deep Water leaving the Atlantic at 30°S. In this study, we use a 15-layer version of this model, identical to that described by Maier-Reimer (1993). The LSG-OGCM velocity fields are taken off line and used in a carbon-cycle model: the Hamburg oceanic carbon cycle model (HAMOCC3), which is also fully documented elsewhere (Heinze et al., 1991; Maier-Reimer, 1993). This model uses the velocity fields to transport important chemical species (principally dissolved inorganic carbon, alkalinity, phosphate, oxygen, and silica) and predicts new production at the ocean surface of calcite, opal, and particulate organic carbon by means of Michaelis-Menten-type production kinetics. Model-derived new production of the three organic particle species (Maier-Reimer, 1993) and model-derived fluxes of material to the seafloor (Heinze et al., 1999) match those observed reasonably well. HAMOCC3 has a grid resolution of 3.5° latitude by 3.5° longitude, giving rise to a total of ≈32,000 wet grid points. It has been modified for this study by the addition of subroutines to describe the behavior of Pb isotopes as described below.

4. MODELLING OF THE ^{210}PB CYCLE

4.1. Oceanic ^{226}Ra Sources

^{226}Ra enters the ocean predominantly by diffusion from bottom sediments (Craig et al., 1973). With a half-life of 1600 yr, ^{226}Ra has been extensively investigated as a potential tracer of ocean circulation, and several surveys of its spatial variation have been performed. For example, ^{226}Ra was measured on 2326 samples during the GEOSECS program (Ostlund et al., 1987) and these measurements used to investigate the potential of ^{226}Ra as an ocean tracer (Bacon et al., 1976; Broecker et al., 1976; Chan et al., 1976; Chung, 1974, 1976, 1981, 1987; Chung et al., 1982; Ku and Lin, 1976; Nozaki and Tsunogai, 1976). We have used these GEOSECS data to construct a dynamically smoothed ^{226}Ra concentration field for the global oceans. Meridianal sections through this field are shown in Figure 1. These show the general increase of ^{226}Ra concentration with depth, reflecting the bottom source and the correlation of ^{226}Ra with deep-water age (Ku and Luo, 1994). Decay of this ^{226}Ra produces 85% of the ^{210}Pb input to the oceans in this model.

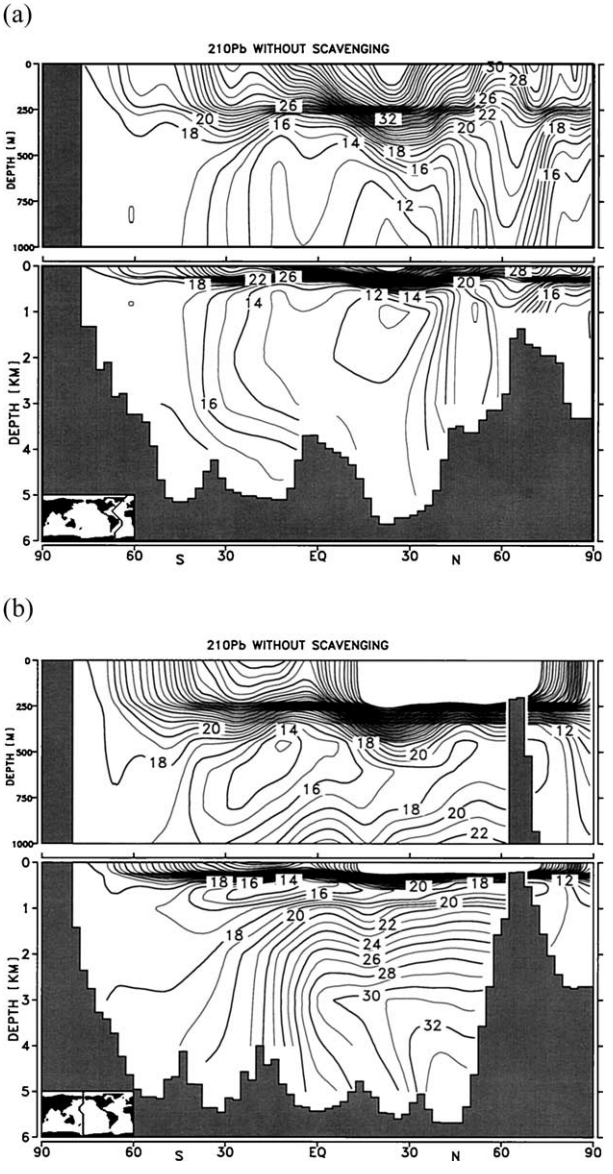

Fig. 3. Expected no-scavenging ^{210}Pb concentrations along meridianal sections in the Atlantic and Pacific Oceans (see inset map for location). Units are dpm/100 L. These figures are model derived and represent the combination of the two sources of ^{210}Pb to the oceans if there were no removal.

4.2. Atmospheric ^{222}Rn Sources

The 15% of ^{210}Pb flux to the oceans not contributed by the decay of ^{226}Ra is due to atmospheric fallout. Gaseous ^{222}Rn escapes from soils to the atmosphere (Graustein and Turekian, 1990), where its short half-life of 3.82 d makes it a potentially useful circulation tracer (Balkanski et al., 1993; Lee and Feichter, 1995). ^{222}Rn decays (via several intermediates, all with half-lives of less than 30 min) to ^{210}Pb, which rapidly adheres to atmospheric particles and is washed from the atmosphere by rain. ^{210}Pb fluxes to the ocean surface are therefore controlled by three factors: proximity to large land masses, atmospheric circulation, and rainfall. For atmosphere-to-ocean ^{210}Pb fluxes in this study, we use the output of an atmospheric model of ^{222}Rn provided by Fritz Zaucker (Lin et al., 1996) (Fig. 2). Atmospheric fallout fluxes of ^{210}Pb in this model agree with the few observations made for open ocean sites (Turekian and Cochran, 1981; Settle et al., 1982; Fuller and Hammond, 1983; Turekian et al., 1983).

4.3. ^{210}Pb Removal

Without removal by particle scavenging, ^{210}Pb activities would be in secular equilibrium with ^{226}Ra in the deep oceans and would be somewhat higher in surface water due to atmospheric rain out (Fig. 3). There have been many studies of ^{210}Pb in the oceans (Bacon et al., 1976; Somayajulu and Craig, 1976; Thomson and Turekian, 1976; Nozaki et al., 1976, 1980, 1991; Bacon, 1977; Chung, 1981, 1987; Spencer et al., 1981; Chung and Craig, 1983; Chung et al., 1983; Cochran et al., 1983; Moore and Smith, 1986; Cochran et al., 1990; Thomson et al., 1993; Anderson et al., 1994; Colley et al., 1995). These studies contain ≈1709 ^{210}Pb measurements for the open ocean, which clearly show the removal of Pb by particle scavenging (compilation available on the Internet at http://www.earth.ox.ac.uk/~gideonh/modelling/u-series.html).

Extensive previous testing of the Hamburg general circulation models (GCMs) used for this study have demonstrated that it generates realistic oceanic distributions of oxygen, phosphate, alkalinity, and, of particular interest for this study, biogenic particles (Maier-Reimer, 1993; Maier-Reimer and Henderson, 1998). We remove ^{210}Pb from the model ocean by irreversible scavenging onto this biogenic particle field. There is also evidence that Pb is removed from the ocean by bottom scavenging to sediment (Spencer et al., 1981), and this removal mechanism is incorporated in the model. This gives two tunable scavenging parameters that can be adjusted to mimic the observed ocean ^{210}Pb distribution: scavenging rate onto biogenic particles, and scavenging rate onto the seafloor. This modeling approach relies on two assumptions about the removal of Pb in the oceans: that it is independent of particle chemistry and that it is irreversible.

To our knowledge, no field or laboratory study has explicitly investigated the effect of particle chemistry on Pb scavenging. Although the Hamburg model generates independent fields of particulate organic carbon, calcite, and opal particle mass, scavenging to each of these particle types at a different rate would increase the tunable parameters from two to four. It is not clear that the available ^{210}Pb observations provide sufficient characteristic variability to enable four tunable parameters to be constrained. We have made some attempts to adjust scavenging rates to the various particle types, but we were not able to significantly improve the quality of the model fit over that using a single rate. In the absence of data to indicate differential scavenging depending on particle chemistry, scavenging onto all particle types equally is therefore most appropriate.

In general, ^{210}Pb activities do not approach ^{226}Ra activities with depth in the oceans as would be expected if Pb scavenging was reversible (i.e., if ^{210}Pb was being removed from surface waters and reequilibrating with deeper waters as for some other metals, notably Th). It is clear from this observation that at least most Pb scavenging is not reversible. We have investigated the possibility that a fraction of Pb removal is reversible within the

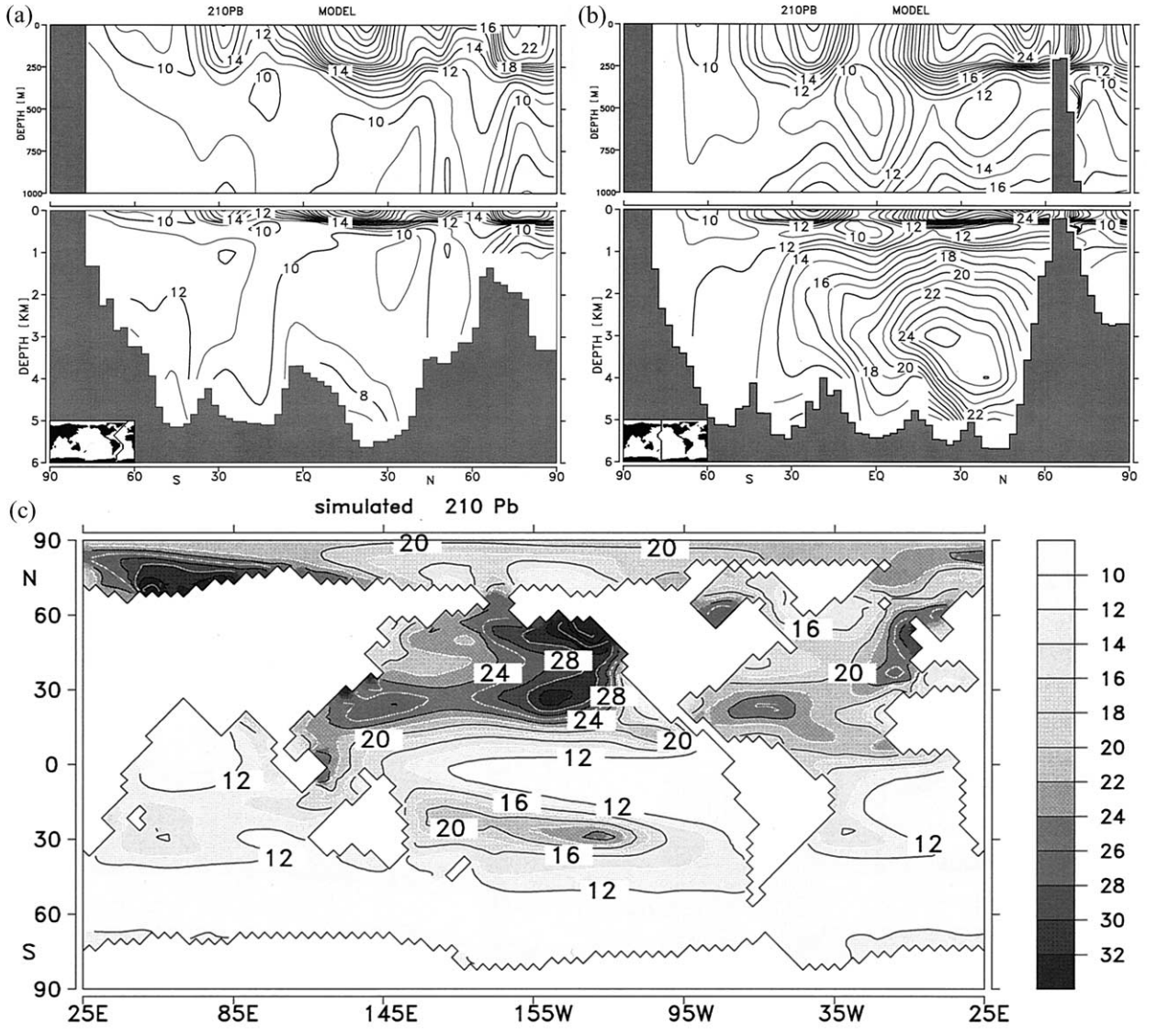

Fig. 4. Model-derived Atlantic and Pacific sections and a surface-water map of ^{210}Pb with scavenging tuned to give the best fit to observed ^{210}Pb values throughout the oceans. Note the lower values than in Figure 3, reflecting the scavenging removal. Units are dpm/100 L.

model but were not able to significantly improve model fit to data by allowing any reversible exchange to occur. We therefore assume that scavenging is fully irreversible. This is in contrast to similar modeling studies for ^{230}Th which required scavenging to be fully reversible (Henderson et al., 1999). Chemically, this difference may reflect the probable ionic speciation of Pb as Pb-carbonate or dichloride complexes (Byrne, 1981), which contrasts with the likely speciation of Th as a neutral hydroxide molecule. It should be noted that irreversible scavenging does not preclude the transport of Pb to depth in the ocean because a large portion of settling particles dissolve while settling, and these release their Pb back into the dissolved phase.

The tuning of the scavenging rates was obtained in a series of 60-yr simulations to minimize the root-mean-square (rms) deviation between observations and model output at the same locations:

$$\text{rms deviation} = \left(\sqrt{\Sigma\,(\text{model}^{210}\text{Pb} - \text{observed}^{210}\text{Pb})^2/\Sigma\,(\text{observed}^{210}\text{Pb})^2}\right) \times 100.$$

The resulting best-fit model yields an rms fit of 4.4 dpm/100 L (disintegrations per minute per 100 litres). This compares with an rms fit of 15.5 dpm/100 L for the no-scavenging model run and a typical measurement uncertainty of 1 to 2 dpm/100 L (Chung et al., 1983). We consider that the best-fit model is removing ^{210}Pb from the oceans in a broadly realistic manner. Resulting meridianal sections and a surface map of ^{210}Pb are shown in Figure 4, and a comparison of the model and observations for the surface layer shown in Figure 5. In general, the model predicts^{210}Pb values in the surface layer well, although model values are slightly high in the Northern Hemisphere. Because this hemisphere has a large continental area, this slight

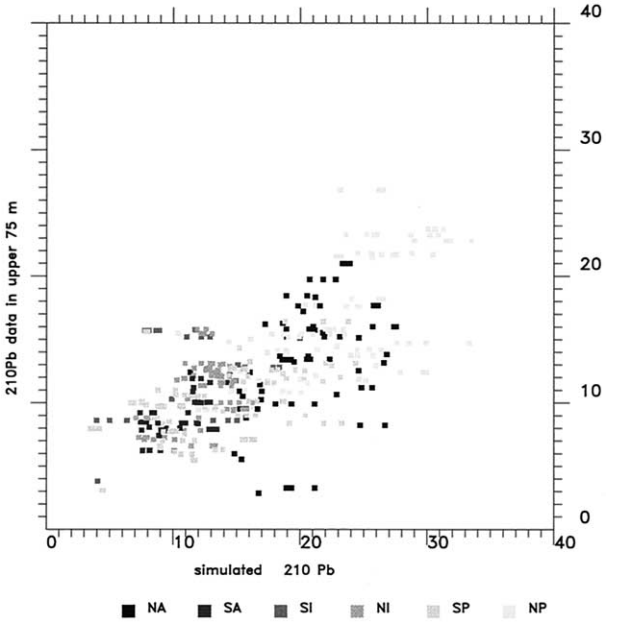

Fig. 5. Comparison of model ^{210}Pb values for the surface ocean with observations. Shading denotes ocean basin (e.g., NA = North Atlantic). Units are dpm/100 L. Note the first-order agreement of model values with observations and the slight overestimates of the model in the Northern Hemisphere.

failing of the model most probably reflects overestimated atmospheric ^{210}Pb fluxes.

Surface-layer ^{210}Pb values without scavenging (Fig. 3) are much higher than observations, so the reasonable replication of observations by the model suggests that it is, on average, removing Pb at a realistic rate from the surface layer. The spatial pattern of this removal can be assessed by comparing ^{210}Pb concentration for the surface layer (Fig. 4) with the measured pattern of Nozaki et al. (1976). First-order features are well captured with the model replicating ^{210}Pb concentrations of ≈25 dpm/100 L for the north Pacific gyre, ≈16 dpm/100 L for the south Pacific gyre, and ≈10 dpm/100 L for the equatorial regions. The details of the east–west distribution are less well replicated, with the model predicting higher ^{210}Pb in the east of the North Pacific, whereas observations suggest higher values in the west. And the model predicts lower ^{210}Pb in the eastern equatorial region, whereas observations suggest that lower values should be in the west. The latter mismatch may be partly due to the paucity of observations in the eastern equatorial region, although the model clearly overestimates absolute values in the western equatorial Pacific, possibly because of inadequate boundary scavenging.

4.4. Residence Times for Pb

The input of ^{210}Pb is well known from observation of the source nuclides. From this input, the model mimics observed ^{210}Pb reasonably well, capturing first-order features of the observed distribution. This suggests that it is removing Pb in a realistic manner. Calculation of residence times for Pb around the oceans can therefore be calculated. Previous residence times for ^{210}Pb have generally been calculated for individual water column profiles with the following equation (Cochran et al., 1990):

$$\tau_{\text{scav}} = \left(\frac{(^{210}\text{Pb supply})}{(^{210}\text{Pb supply}) - (^{210}\text{Pb observed})} - 1 \right) \times \frac{1}{\lambda_{210}},$$

where τ_{scav} is the residence time relative to scavenging, and λ_{210} is the half-life of ^{210}Pb. In the one-dimensional situation of a single profile, ^{210}Pb supply is given simply by

$$(^{210}\text{Pb supply}) = (^{226}\text{Ra}) + (^{210}\text{Pb settling}),$$

where ^{210}Pb settling is the ^{210}Pb released to the dissolved phase from above, either by atmospheric fallout, or by dissolution of settling particles. This equation, however, makes no allowance for advection of ^{210}Pb into or out of the water column. To consider the true three-dimensional case, advection terms must be added. As an extreme example, consider a packet of water advected quickly from an area of high productivity to one of low productivity. ^{210}Pb scavenging in the high-productivity region will reduce the ^{210}Pb/^{226}Ra ratio beneath equilibrium. This ratio will be advected to the region of low productivity where, even if ^{210}Pb removal is nonexistent, the low observed ^{210}Pb would suggest a one-dimensional residence time similar to that in the high-productivity region.

Because the use of stable Pb isotopes in the oceans as paleotracers is of interest, we wish to learn about the rate and distribution of Pb removal. A more appropriate way of assessing Pb residence times, therefore, is to calculate τ_{scav} from the output of Pb at each grid point rather than the inputs:

$$\tau_{\text{scav}} = \frac{\text{water column Pb inventory}}{\text{removal rate of Pb}}$$

Maps of τ_{scav} calculated in this way for Pb scavenging from the upper 75 m and upper 2000 m of the water column are shown in Figure 6. The removal rate of Pb is assessed from ^{210}Pb removal, but τ_{scav} is calculated in these figures by using stable Pb isotopes as these are of interest as paleotracers. The slight difference in water-column profiles between ^{210}Pb and stable Pb will lead to slight differences in τ_{scav} for these two types of Pb but these differences will be subtle and the maps in Figure 6 can be considered as representing both radioactive and stable Pb. Average values of τ_{scav} are similar to those in previous studies, but the degree of variability is higher, reflecting the calculation from removal rather than input. This difference in calculation method also makes it difficult to directly compare τ_{scav} values calculated from ^{210}Pb at individual sites with τ_{scav} calculated from the model. Nevertheless, model τ_{scav} agrees well with observations in areas such as South Africa (5 yr, Shannon et al., 1970) and the Labrador Sea (6 yr, Bacon et al., 1978). Estimates of τ_{scav} that use the removal of the anthropogenic Pb pulse at Bermuda are ≈2 yr (Sherrell and Boyle, 1992), which the model predicts well.

The model predicts variability in τ_{scav} of more than an order of magnitude, reflecting the dramatic changes in biogenic particle flux observed around the oceans. The large variability in τ_{scav} when calculated from the Pb removal flux will serve to increase provinciality in Pb isotopes with regions relatively isolated by high-productivity belts. The global average Pb

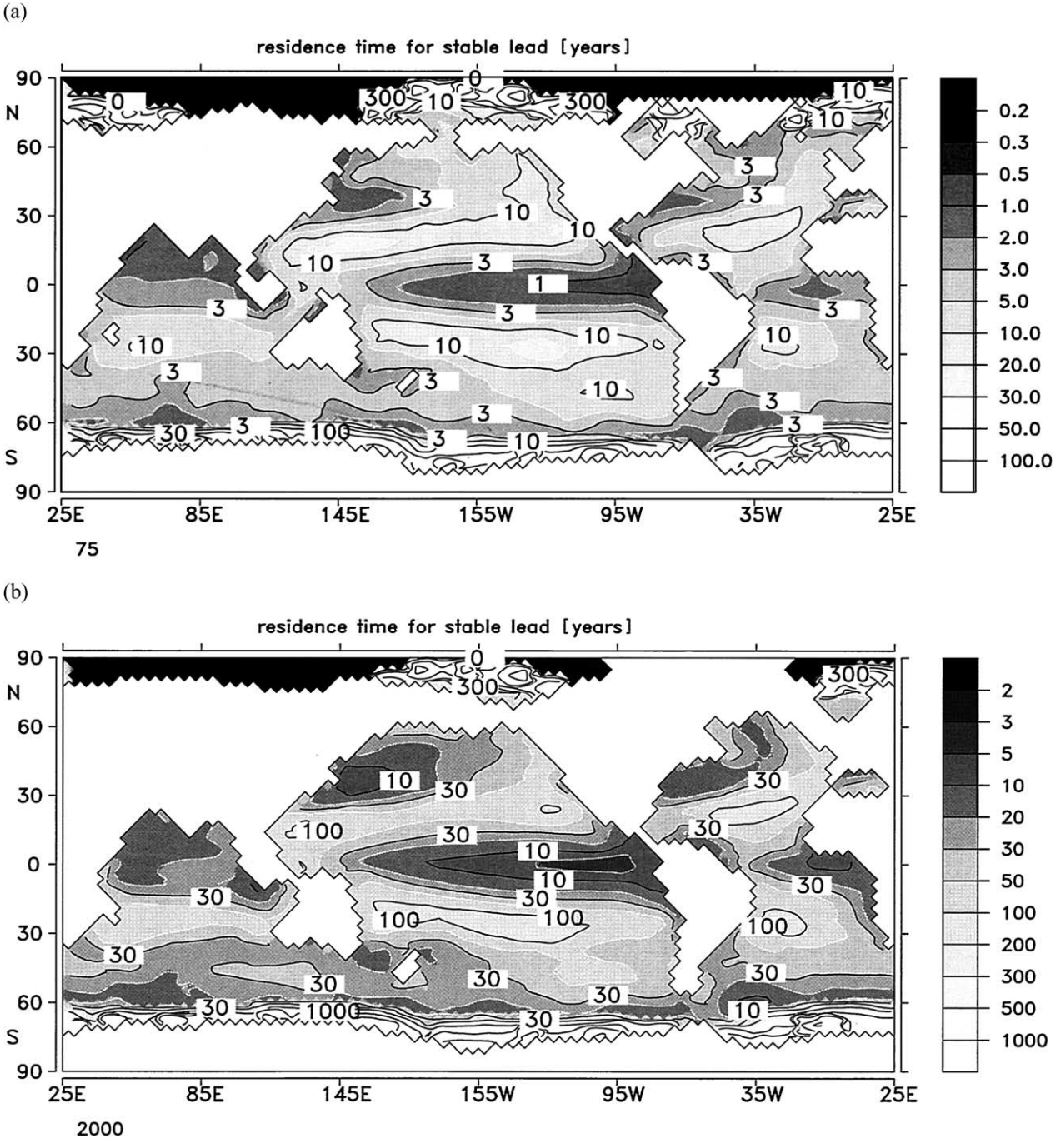

Fig. 6. Residence times for Pb based on the best fit model of ^{210}Pb removal. These are calculated as the water column inventory of Pb above a horizon divided by the flux of Pb through that horizon. Residence time for Pb (a) above 75 m and (b) above 2000 m. Units are years.

residence time for the model (e.g., the total ocean Pb inventory divided by Pb output due to scavenging) is 48 yr.

5. MODELING OF THE STABLE PB CYCLE

The flow fields of the GCM advect Pb, and the ^{210}Pb distribution constrains the removal of Pb, so we can now begin to investigate the behavior of natural, stable Pb in the ocean. The missing part of the puzzle is the pattern of inputs of stable Pb. For this study, we have chosen a highly simplified pattern of inputs (Table 1). It should be stressed that this simplified input is not intended to be a fully accurate representation of Pb input to the oceans but instead is focused on answering some basic questions about the control of open-ocean Pb isotopes.

Table 1. Simplified stable-Pb-isotope input for the model. Isotope ratios are taken from the literature. River values are based on river particulates or fan turbidites. Fluxes are estimated using approaches outlined in the text.

Site	Total Pb flux (%)	Pb flux (10^9 g/yr)	$^{206}Pb/^{204}Pb$	Reference for isotope ratios
Rivers Yangtze	24	3.1	18.40	Hemming and McClenan, 2001
Amazon	23	3.0	18.91	Asmeron and Jacobson, 1993 White and Dupre, 1985
Ganges	14	1.8	18.83	Hemming and McClenan, 2001
Russian Rivers	11	1.8	19.20	Estimated
Mississippi	13	1.7	19.18	Asmeron and Jacobson, 1993
Total rivers	88	11.4		
Eolian Sahara			18.98	Hamelin et al., 1989
Patagonia			18.18	Grousset et al., 1992
Australia			18.75	Grousset et al., 1992
China			18.81	Jones et al. 2000
S. Africa			18.80	Grousset et al., 1992
Arabia			18.60	Estimated
Total eolian	12	1.6		

5.1. Dust Inputs of Pb

The size of eolian inputs of dissolved Pb to the oceans relative to riverine inputs is key to the question of which of these Pb sources control the open-ocean Pb-isotope signal. The simplest way of assessing the relative size of the dust contribution to oceanic Pb is from the total annual output flux of authigenic Pb which equals 6.3×10^7 mol/yr ($=1.3 \times 10^{10}$ g/yr) (Chow and Patterson, 1962). The total flux of eolian material to the oceans is $\approx 1 \times 10^{15}$ g/yr (Duce et al., 1991). Assuming that this is typical crustal material with a Pb concentration of 1×10^{-7} mol/g ($=$20ppm) and that 8% of this dust dissolves in seawater (by analogy with Al; Maring and Duce, 1987), a total eolian contribution to the dissolved Pb budget of 7.7×10^6 mol/yr ($=1.6 \times 10^9$ g/yr) is suggested, or 12% of the required natural annual budget. Uncertainty in this value arises principally from the assumption that 8% of the Pb is released from dust to the dissolved phase. This value is reasonable given the well-constrained 8% value for Al, which represents a good tracer for continental silicates. But there remains the possibility that a surface coating rich in Pb in typical dust might increase the dissolvable percentage of Pb. If the true release of Pb is higher than the modeled 8% dissolution, this will lead to an increasing significance for dust in controlling open-ocean Pb values. For small changes, the influence of dust on open-ocean Pb will scale approximately linearly with dissolution percentage.

The pattern of eolian inputs to the ocean is easier to constrain. There are several models of global dust fluxes that accurately replicate observations. For this study, we use the model of Andersen et al. (1998), which has two particular advantages. First, it discriminates between dust from different sources, allowing us to label various dust sources with different Pb isotope signals. And second, there is a glacial version of the model that allows us to investigate past variability. The distribution of dust fluxes to the ocean for the Holocene and last glacial maximum based on this model are shown in Figure 7.

5.2. Riverine Inputs of Pb

The 88% of dissolved Pb that is not supplied by dust dissolution must be supplied by riverine inputs. This is despite the fact that Pb removal is expected to occur in the nearshore environment and suggests that original riverine Pb fluxes must be even larger before this removal. For the model, we characterize this riverine Pb input crudely by using five-point sources of dissolved Pb representing five important rivers. These sources are selected as representing the largest contributors of total dissolved load (TDL) to each of the major oceans (Berner and Berner, 1987). Between them, these rivers represent $\approx$25% of the total flux of TDL to the ocean. Dissolved Pb fluxes for the rivers are scaled relative to one another according to TDL (Table 1) and are input directly to the open ocean, thereby assuming that estuarine loss is the same for all the river systems. To a first approximation, it is sensible to scale rivers by using their TDL because in pristine streams where anthropogenic Pb contributions are minimal, dissolved Pb behaves similarly to iron (Erel and Morgan, 1992) and Fe concentrations in rivers correlate reasonably with TDL (Goldstein and Jacobsen, 1987).

The issue of estuarine loss of Pb is complex and varies with the estuary studied. In some rivers, Pb is removed by estuarine processes—for example, the Seine (Chiffoleau et al., 1994), the Savannah (Windom et al., 1985), the Gota (Danielsson et al., 1983), and the Bang Pakong (Windom et al., 1988). In other rivers, Pb behaves conservatively—for example, the Rhone (Elbaz-Poulichet et al., 1996), the Ogeechee (Windom et al., 1985), and several Texas rivers (Benoit et al., 1994). And in some examples, Pb is released during transit through the estuary, as in the Loire (Boutier et al., 1993), or is seen to undergo both removal and release, as in the Gironde (Elbaz-Poulichet et al., 1984). This degree of complexity and the lack of measurements on major river systems means that differential estuarine removal cannot be incorporated in the model at this stage.

5.3. Natural Seawater Pb Concentrations

Model-derived seawater Pb concentrations for the natural system without anthropogenic inputs average 2.2 pmol/kg ($=$0.45 ng/kg) (Fig. 8). This average Pb concentration is controlled by the annual input ($=$output at steady state) and the residence time. Because the residence time is well constrained by the ^{210}Pb data, the average Pb concentration is as accurate

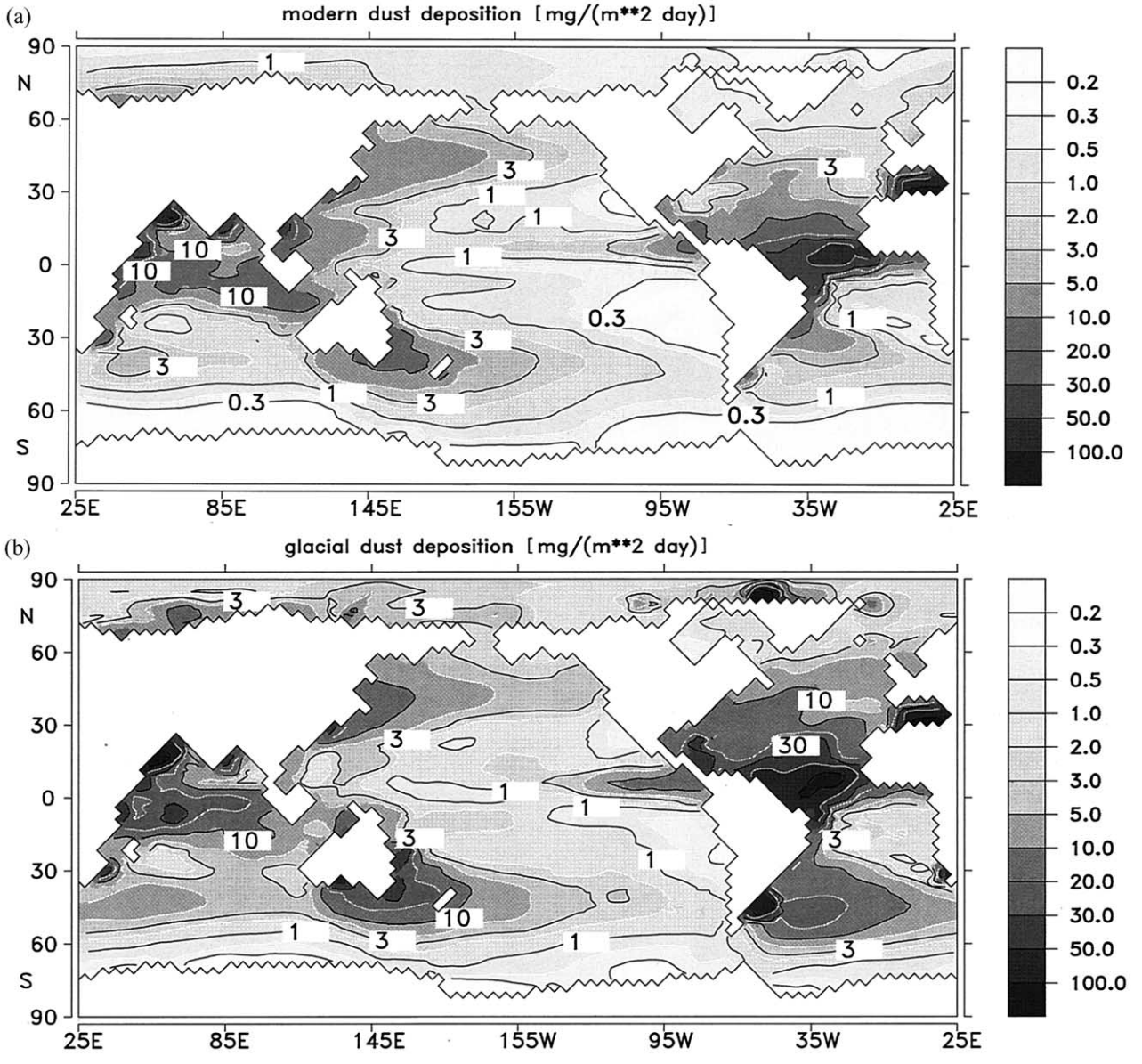

Fig. 7. Dust input to the surface of the oceans. Values are mg/(m^2d). Values are taken from a model by Andersen et al. (1998). (a) Modern fluxes. (b) Expected fluxes at the last glacial maximum.

as the estimate of total Pb output of 6.3×10^7 mol/yr (Chow and Patterson, 1962) and will scale linearly with any changes in this value.

Expected natural Pb concentrations are generally at a maximum in the surface ocean (Fig. 8). This should not be a surprise given that riverine and eolian sources of Pb are input into the surface ocean and given that scavenging is irreversible. Nevertheless, it is interesting that the present-day surface-water Pb concentration peak is not solely due to anthropogenic Pb input, as has commonly been assumed. This model result is considered reasonably robust. Only a large fraction of reversible scavenging would remove the natural surface maximum, and this seems unlikely given the inability to mimic ^{210}Pb profiles with reversible exchange.

Natural seawater Pb concentrations are about an order of magnitude higher in the Northern Hemisphere than in the Southern Hemisphere (Fig. 8). This result is entirely dependent on the assumed input of stable Pb. Although the input used here is simplistic, it does seem likely that inputs to the Northern Hemisphere will dominate the natural Pb budget due to larger area of continents in that hemisphere. The difference between the hemisphere Pb concentrations are exaggerated by the dramatically increased scavenging of Pb in the high productivity equatorial belts. This is particularly marked in the Pacific section, where the majority of the Pb concentration change occurs between 20°N and the equator. Finer details of the stable Pb concentration sections shown in Figure 8 are not expected to be accurate due to the simplistic inputs used in this study. But the length scales of change are expected to be broadly correct for seawater Pb concentrations.

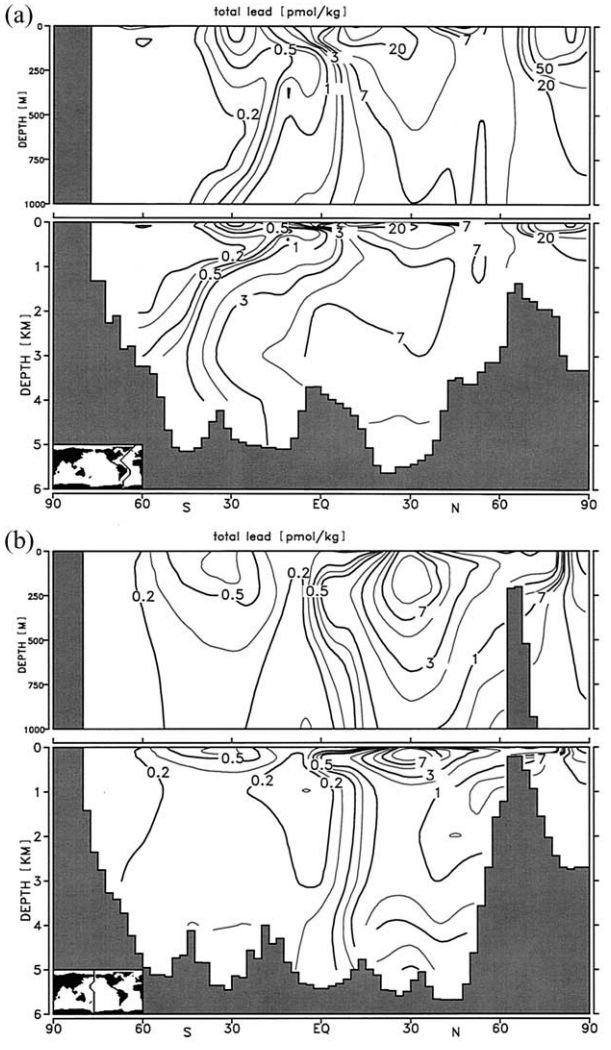

Fig. 8. Atlantic and Pacific sections of stable Pb concentrations. Units are pmol/kg (1 pmol/kg = 0.21 ng/kg) and are based on a total input of stable Pb of 6.3×10^7 mol/yr (Chow and Patterson, 1962). Precise values are not expected to be accurate because of the simplistic input pattern of Pb, but the average concentration is expected to be accurate. The length scale of changes in concentration is also expected to be broadly correct, and the general pattern of higher values in the Northern Hemisphere is probably correct on the basis of the presence of more continental area there.

5.4. Influence of a Point Source

The influence of a point source of Pb is illustrated here by model results for the Amazon River source of stable Pb (Fig. 9). In the model, the Amazon contributes 23% of the total open ocean Pb budget. This is sufficient for it to play a large role in the surface Atlantic north of ≈20°S. Amazon Pb is advected to depth with NADW and is a significant portion of seawater Pb throughout the deep Atlantic. During this transport, however, the total Pb concentration is reduced by an order of magnitude so that once into the Indian ocean, the influence of Amazon Pb is rapidly reduced by mixing with other sources, notably the Ganges/Brahmaputra. Once into the Pacific, the influence of the Amazon is expected to be small and is less than 10% throughout the water column in the model ocean for all latitudes north of ≈60°S.

Again, precise features of the influence of Amazon Pb are not expected to be accurately represented by the model, given the crude input pattern of stable Pb. But the general length scale over which a point source of Pb will influence seawater isotopic balance is expected to be a robust feature. This result is encouraging for the use of Pb isotopes as an oceanic tracer because the expected advection of isotope signals is long enough to allow them to be accurately reconstructed, but short enough to prevent full mixing of the isotope signal.

5.5. Riverine vs. Dust Control of the Open Ocean

With the stable-Pb inputs assumed in this model, dust contributes between 5 and 90% of the fraction of seawater Pb around the ocean (Fig. 10). The influence of dust is at its highest in the surface waters of the Southern Ocean, where it contributes up to 90% of the seawater Pb. Although this result is dependent on the distribution of stable Pb inputs to the oceans, large inputs of riverine Pb to the Southern Ocean are unlikely, so the dust-dominated signal seen in the model ocean is very likely to be a feature of the natural Pb pattern. This situation is also true in the deep waters of the Southern Ocean, where eolian Pb makes a lesser but still important contribution to modeled seawater Pb (Fig. 10). This importance of dust for large portions of the Pacific is in agreement with the study of Jones et al. (2000), based on measured dust isotope compositions.

Elsewhere in the model ocean, particularly close to the assumed riverine inputs, the influence of dust Pb is lower but is never completely swamped by riverine inputs. It seems a robust conclusion of the model that both dust and riverine sources of Pb are important in setting the Pb-isotope composition of seawater. Unless the eolian fraction of Pb sources, assumed to be 12% for this model, is dramatically in error, both sources must play a role. This points to the importance of three-dimensional modeling as a necessary tool to fully understand the oceanic Pb cycle.

6. STABLE PB ISOTOPES

To assess changes in the distribution of ocean Pb isotopes during glacial–interglacial cycles, we have assigned each of the sources of Pb a $^{206}Pb/^{204}Pb$ on the basis of literature data (Table 1). This enables calculation of the distribution of $^{206}Pb/^{204}Pb$ in the model ocean (Fig. 11) and a comparison of this distribution with that observed. Several studies have reported Pb-isotope data from Mn crust surfaces, and these are expected to represent the bottom water dissolved Pb-isotope composition for the ocean before anthropogenic contamination. A collation of such data provides 151 observations (Chow and Patterson, 1959, 1962; Reynolds and Dasch, 1971; O'Nions et al., 1978; Abouchami and Goldstein, 1995; von Blanckenburg et al., 1996). These data are too sparse to enable a full contour map to be drawn, but the observed $^{206}Pb/^{204}Pb$ is plotted as a shaded point map in Figure 11.

Although the input of stable Pb to the model ocean is simplified, first-order features in the model $^{206}Pb/^{204}Pb$ map reproduce those observed well. Model values in the northern

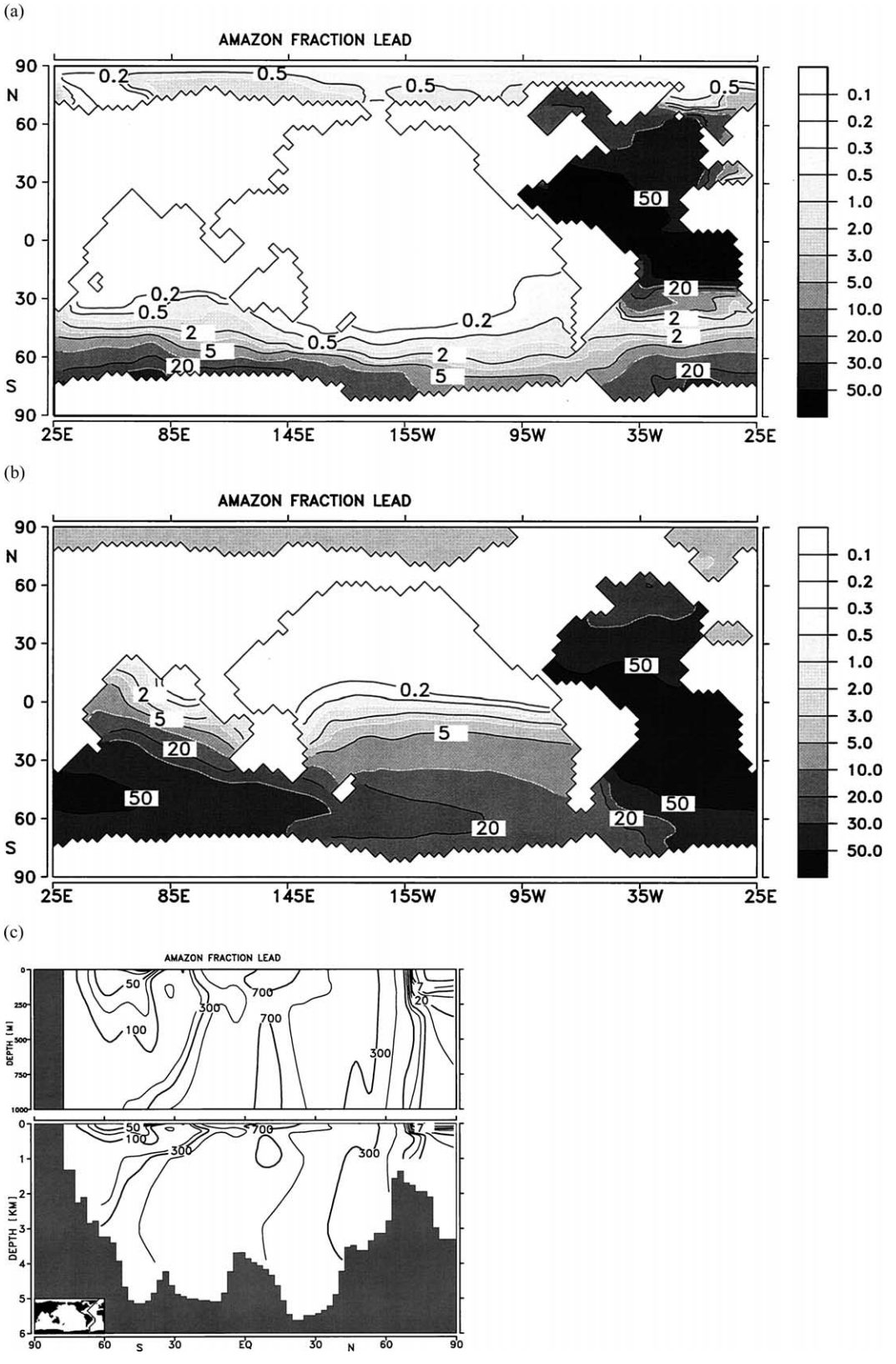

Fig. 9. Model-derived surface-ocean map, deep-ocean map (2000 m), and Atlantic Ocean section to show the influence of the Amazon River source of Pb on the Pb inventory of seawater. These maps are based on a simplified pattern of Pb inputs to the oceans but nevertheless provide an indication of the distance that a Pb-isotope signal is expected to be advected in the oceans. Units are % of total seawater Pb; a value of 50 indicates that half of the Pb at that location came from the Amazon.

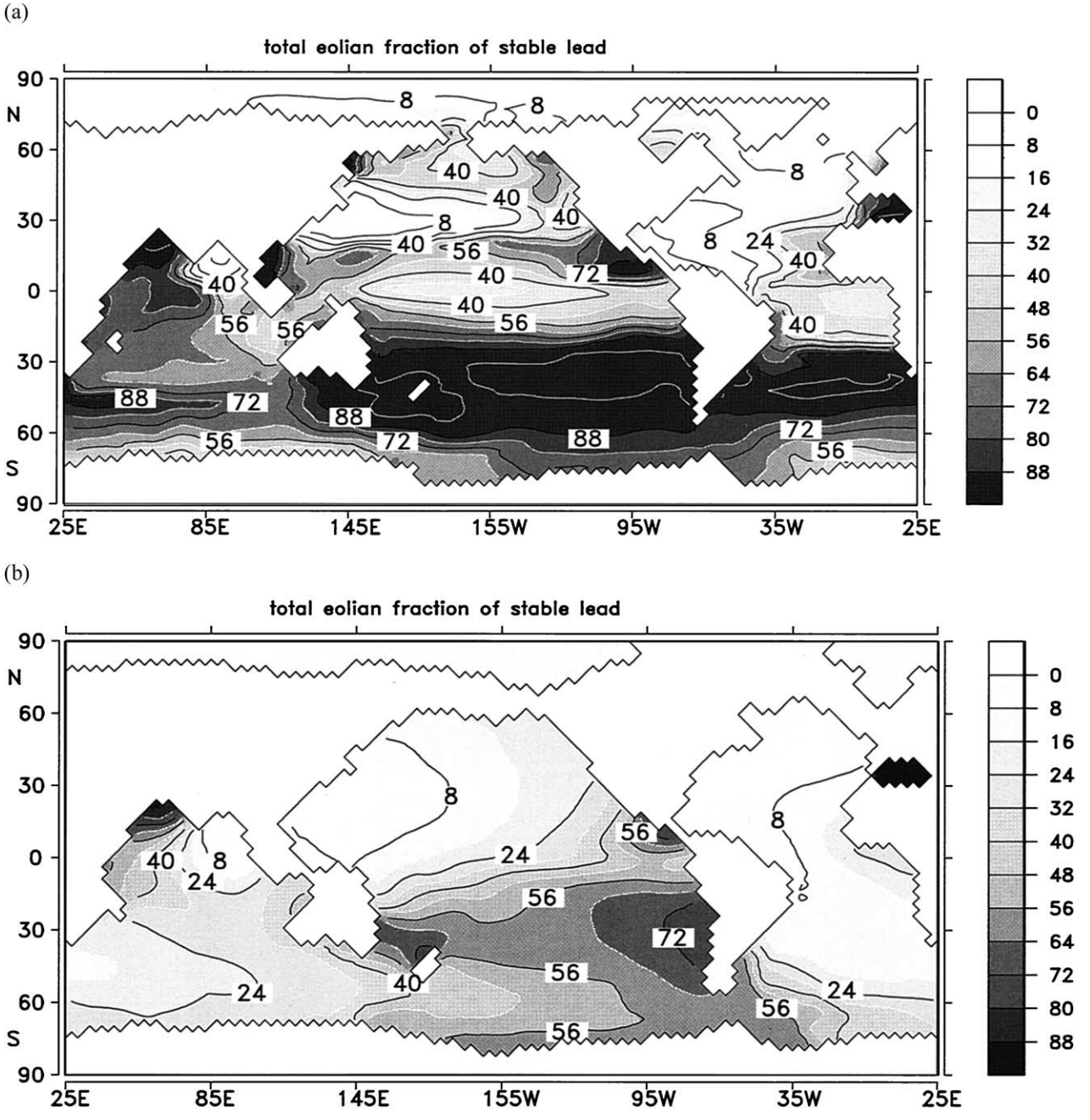

Fig. 10. Model-derived maps of a) surface ocean and b) deep ocean (2000 m) to show the influence of the eolian sources of Pb on the Pb inventory of seawater. These maps are based on a heavily simplified pattern of Pb inputs to the oceans but nevertheless provide an indication of the eolian source in controlling the Pb isotope ratio of open ocean waters. Units are in % of total seawater Pb; a value of 50 means that half of the Pb at that location is from an eolian source.

section of each ocean basin are close to those observed; the general meridianal structure in each ocean is correct, and the tongue of high ratios seen across the Southern Indian Ocean is reproduced. The biggest failure of the model is that it does not capture observed smaller-scale Pb-isotope variability, particularly in the Southern Ocean. Most particularly, it does not capture the high $^{206}Pb/^{204}Pb$ values observed at 130°W. These values occur where the model predicts that more than 50% of deep-water Pb is derived from dust. This may reflect fractionation of Pb isotopes during dust transport processes, or a more complex pattern of source isotope ratios than has been included in the model. Despite this failing, the ability of the model to capture first-order features of the global stable-Pb-isotope distribution is encouraging.

Given this success, the model can be used to assess the expected sensitivity of the ocean Pb-isotope distribution to changes in the past environment. We have performed a glacial simulation via model flow fields optimized for glacial surface

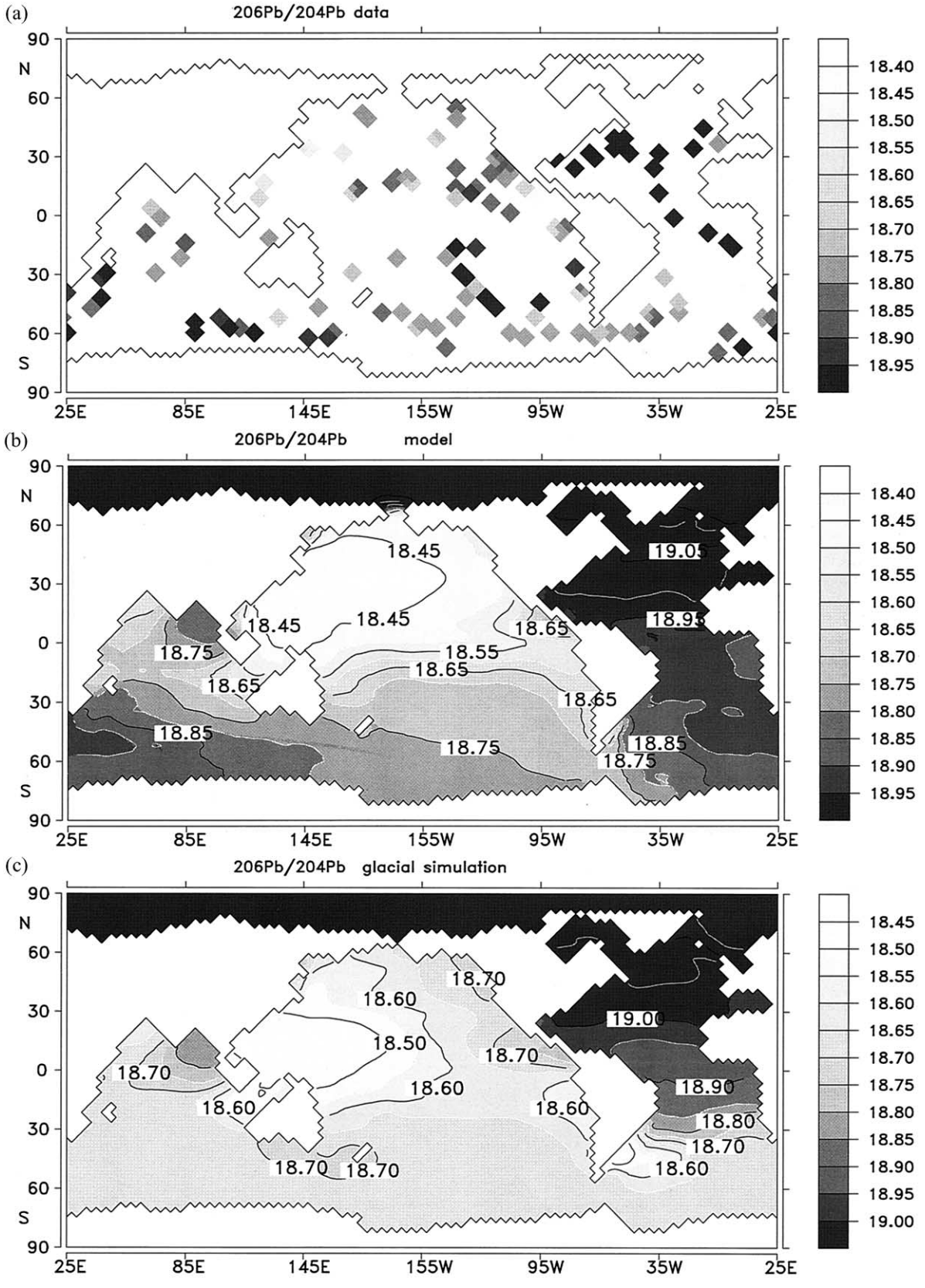

Fig. 11. a) Observed $^{206}Pb/^{204}Pb$ values from Mn crusts compared to, b) Holocene model reconstruction and, c) last glacial maximum model reconstruction.

salinity (Winguth et al., 1999). Ocean circulation in this model reproduces the main features of glacial $\delta^{13}C$ and reduces NADW by about half, in line with expectations (Winguth et al., 1999). Pb was input to the glacial model from the same sources and with the same isotope ratios as in the Holocene run. Fluxes of riverine Pb were maintained at the Holocene level as present estimates suggest that continental erosion rates did not change significantly from glacial to interglacial times (Henderson et al., 1994). Fluxes of eolian material to the oceans are thought to have increased significantly, however, and Pb fluxes were increased to reflect this. The glacial dust field of Andersen et al. (1998) was used to constrain aerosol Pb input, representing a 1.9 times greater flux than for the interglacial run (Fig. 7).

$^{206}Pb/^{204}Pb$ remains largely unchanged in the glacial run close to the riverine inputs (Fig. 11). But further from these inputs significant changes in ratio are observed, particularly in the Southern Ocean and the northeast Pacific Ocean. The glacial model demonstrates that even relatively small changes in boundary conditions can produce significant changes in the Pb-isotope pattern, as long as a sensitive area of the oceans is selected. Larger changes in environment, such as changes in riverine input or circulation changes in response to opening or closing gateways, are obviously expected to have a greater effect.

7. CONCLUSIONS

By taking existing data sets for the sources of ^{210}Pb, a three-dimensional ocean model is able to predict observed ^{210}Pb values reasonably well, suggesting that the model realistically mimics advection and removal of Pb. Collating data in a global model in this way allows globally averaged values to be calculated for factors that have only previously been assessed on a local or regional scale. The model suggests that 85% of ^{210}Pb input to the global ocean is from ^{226}Ra decay, with only 15% from atmospheric fallout. The global average residence time for Pb, assessed from the model, is 48 yr. And by using a previously measured value for the stable-Pb output flux, the average Pb concentration of ocean water before human influence is assessed from the model to be 2.2 pmol/kg.

This modeling also allows spatial patterns of stable Pb concentration to be assessed. The model suggests that Pb residence times vary spatially by more than an order of magnitude. This would increase provinciality of Pb isotopes in the oceans separated by belts of high productivity with rapid Pb removal. From arguments that stable Pb is input to the oceans by dust and rivers, coupled with the fact that modeling suggests largely irreversible scavenging of Pb, a near-surface maximum in Pb concentration is expected even in the natural Pb cycle. The assumption that dust and rivers are the inputs for stable Pb also leads the model to predict 10 times higher average Pb concentrations in the Northern Hemisphere than the Southern Hemisphere, reflecting the larger continental sources in the north.

Finally, the model enables an assessment of which sources control open-ocean Pb isotopes. Point sources of Pb are expected to represent only $\approx$10% of the total seawater Pb inventory by the time they are advected from the ocean basin into which they flow, providing Pb-isotope signals with a suitable length scale of advection to act as ocean circulation tracers. From arguments that 12% of the Pb contributed to the oceans globally comes from dust dissolution, the model suggests that Pb from dust represents about half of the total Pb inventory for much of the Southern Ocean. Changes in model boundary conditions also suggest that Pb isotopes are expected to vary significantly, even for reasonably minor changes

The limitations of the model presented here are largely due to poor knowledge of the inputs of natural stable Pb to the oceans. It is unlikely that such inputs can be directly measured due to the extreme anthropogenic perturbation of the Pb cycle. Mn-crust studies of the preanthropogenic Pb isotope distribution have recently improved, both in spatial coverage and in analytical precision. It is hoped that the use of three-dimensional models will enable these data sets to be used to reconstruct preanthropogenic sources of Pb to the oceans. This knowledge may then fully unlock the potential of Pb isotopes to provide information about past weathering fluxes and ocean circulation.

Acknowledgments—We thank Wally Broecker for discussion of the approach used here. We are grateful to Katrin Andersen and Fritz Zaucker for providing model output of dust and atmospheric fluxes, respectively. We also thank Wafa Abouchami, Ed Boyle, and Russ Flegal for full and constructive reviews that significantly improved the manuscript.

Associate editor: R. H. Byrne

REFERENCES

Abouchami W. and Goldstein S. L. (1995) A lead isotopic study of circum–Antarctic manganese nodules. *Geochim. Cosmochim. Acta* **59,** 1809–1820.

Abouchami W., Goldstein S. L., Galer S. J. G., Eisenhauer A., and Mangini A. (1997) Secular changes of lead and neodymium in central Pacific seawater recorded by a Fe-Mn crust. *Geochim. Cosmochim. Acta* **61,** 3957–3974.

Andersen K. K., Armengaud A., and Genthon C. (1998) Atmospheric dust under glacial and interglacial conditions. *Geophys. Res. Lett.* **25,** 2281–2284.

Anderson R. F., Fleisher M. Q., Biscaye P. E., Kumar N., Dittrich B., Kubik P., and Suter M. (1994) Anomalous boundary scavenging in the Middle Atlantic Bight: Evidence from ^{230}Th, ^{231}Pa, ^{10}Be and ^{210}Pb. *Deep-Sea Res.* **41,**537–561.

Asmeron Y. and Jacobson S. B. (1993) The Pb isotopic evolution of the Earth: Inferences from river water suspended loads. *Earth Planet. Sci. Lett.* **115,** 245–256.

Bacon M. P. (1977) ^{210}Pb and ^{210}Po results from F.S. "Meteor" cruise 32 in the North Atlantic. *"Meteor" Forsch.-Ergebnisse* **19(A),**24–36.

Bacon M. P., Spencer D. W., and Brewer P. G. (1976) $^{210}Pb/^{226}Ra$ and $^{210}Po/^{210}Pb$ disequilibria in seawater and suspended particulate matter. *Earth Planet. Sci. Lett.* **32,** 277–296.

Bacon M. P., Spencer D. W., and Brewer P. G. (1978) Lead-210 and polonium-210 as marine geochemical tracers: Review and discussion of results from the Labrador Sea. In *Natural Radiation Environment III*, Vol. 1 (eds. T. F. Gesell and W. F. Lower), pp. 473–501. U.S. Department of Energy.

Balkanski Y. J., Jacob D. J., Gardner B. M., Graustein W. C., and Turekian K. K. (1993) Transport and residence times of tropospheric aerosols inferred from a global 3-dimensional simulation of Pb-210. *J. Geophys. Res.* **98(D11),** 20573–20586.

Benoit G., Oktay-Marshall S. D., Cantu A., Hood E. M., Coleman C. H., Corapcioglu M. O., and Santschi P. H. (1994) Partitioning of Cu, Pb, Ag, Zn, Al, and Mn between filter-retained particles, colloids, and solution in six Texas estuaries. *Mar. Chem.* **45,** 307–336.

Berner E. K. and Berner R. A. (1987) *The Global Water Cycle: Geochemistry and Environment.* Prentice-Hall.

Boutier B., Chiffoleau J. F., Auger D., and Truguet I. (1993) Influence

of the Loire River on dissolved lead and cadmium concentrations in coastal waters of Brittany. *Estuar. Coastal Shelf Sci.* **36,** 133–145.
Broecker W. S., Godard J., and Sarmiento J. (1976) The distribution of ^{226}Ra in the Atlantic ocean. *Earth Planet. Sci. Lett.* **32,** 220–235.
Byrne R. H. (1981) Inorganic lead complexation in natural seawater determined by UV spectroscopy. *Nature* **290,** 487–489.
Chan L. H., Edmond J. M., Stallard R. F., Broecker W. S., Chung Y. C., Weiss R. F., and Ku T. L. (1976) Radium and barium at GEOSECS stations in the Atlantic and Pacific. *Earth Planet. Sci. Lett.* **32,** 258–267.
Chen J. H., Wasserburg G. J., Von Damm K. L., and Edmond J. M. (1986) The U-Th-Pb systematics in hot springs on the East Pacific Rise at 21°N and Guaymas Basin. *Geochim. Cosmochim. Acta* **50,** 2467–2479.
Chiffoleau J.-F., Cossa D., Auger D., and Turquet I. (1994) Trace metal distribution, partition and fluxes in the Seine estuary (France) in low discharge regime. *Mar. Chem.* **47,** 145–158.
Chow T. J. and Patterson C. C. (1959) Lead isotopes in manganese nodules. *Geochim. Cosmochim. Acta* **17,** 21–31.
Chow T. J. and Patterson C. C. (1962) The occurrence and significance of Pb isotopes in pelagic sediments. *Geochim. Cosmochim. Acta* **26,** 263–308.
Christensen J. N., Halliday A. N., Godfrey L. V., Hein J. R., and Rea D. K. (1997) Climate and ocean dynamics and the lead isotopic records in Pacific ferromanganese crusts. *Science* **277,** 913–918.
Chung Y.-C. (1974) Radium-226 and Ra-Ba relationships in Antarctic and Pacific waters. *Earth Planet. Sci. Lett.* **23,** 125–135.
Chung Y.-C. (1976) A deep ^{226}Ra maximum in the northeast Pacific. *Earth Planet. Sci. Lett.* **32,** 249–257.
Chung Y. (1981) ^{210}Pb and ^{226}Ra distributions in the circumpolar waters. *Earth Planet. Sci. Lett.* **55,**205–216.
Chung Y. (1987) ^{210}Pb in the western Indian Ocean: Distribution, disequilibrium, and partitioning between dissolved and particulate phases. *Earth Planet. Sci. Lett.* **85,** 28–40.
Chung Y., Finkel R. C., and Kim K. (1982) ^{226}Ra, ^{210}Pb and ^{210}Po in the Red Sea. *Earth Planet. Sci. Lett.* **58,** 213–224.
Chung Y. and Craig H. (1983) ^{210}Pb in the Pacific: The GEOSECS measurements of particulate and dissolved concentrations. *Earth Planet. Sci. Lett.* **65,** 406–432.
Chung Y., Finkel R., Bacon M. P., Cochran J. K., and Krishnaswami S. (1983) Intercomparison of ^{210}Pb measurements at GEOSECS station 500 in the northeast Pacific. *Earth Planet. Sci. Lett.* **65,** 393–405.
Cochran J. K., Bacon M. P., Krishnaswami S., and Turekian K. K. (1983) ^{210}Po and ^{210}Pb distributions in the central and eastern Indian ocean. *Earth Planet. Sci. Lett.* **65,** 433–452.
Cochran J. K., McKibbon-Vaughan T., Dornblaser M. M., Hirschberg D., Livingston H. D., and Buesseler K. (1990) ^{210}Pb scavenging in the North Atlantic and North Pacific oceans. *Earth Planet. Sci. Lett.* **97,** 332–352.
Colley S., Thomsom J., and Newton P. P. (1995) Detailed ^{230}Th, ^{232}Th and ^{210}Pb fluxes recorded by the 1989/90 BOFS sediment trap time-series at 48°N, 20°W. *Deep-Sea Res.* **42(6),** 833–848.
Craig H., Krishnaswami S., and Somayajulu B. L. K. (1973) ^{210}Pb-^{226}Ra: Radioactive disequilibrium in the deep sea. *Earth Planet. Sci. Lett.* **17,** 295–305.
Danielsson L.-G., Magnusson B., Westerlund S., and Zhang K. (1983) Trace metals in the Gota estuary. *Estuar. Coastal Shelf Sci.* **17,** 73–85.
Duce R. A., Liss P. S., Merrill J. T., Atlas E. L., Buat-Menard P., Hicks B. B., Miller J. M., Prospero J. M., Arimoto R., Church T. M., Ellis W., Galloway J. N., Hansen L., Jickells T. D., Knap A. H., Reinhardt K. H., Schneider B., Soudine A., Tokos J. J., Tsunogai S., Wollast R., and Zhou M. (1991) The atmospheric input of trace species to the world ocean. *Global Biogeochem. Cycles* **5(3),** 193–259.
Elbaz-Poulichet F., Holliger P., Huang W. W., and Marin J.-M. (1984) Lead cycling in estuaries, illustrated by the Gironde estuary, France. *Nature* **308,** 409–414.
Elbaz-Poulichet F., Garnier J.-M., Guan D. M., Martin J.-M., and Thomas A. J. (1996) The conservative behavior of trace metals (Cd, Cu, Ni and Pb) and As in the surface plume of the stratified estuaries: Examples of the Rhone river (France). *Estuar. Coastal Shelf Sci.* **42,** 289–310.
Erel Y. and Morgan J. J. (1992) The relationship between rock-derived lead and iron in natural waters. *Geochim. Cosmochim. Acta* **56,** 4157–4167.
Flegal A. R., Itoh K., Patterson C. C., and Wong C. S. (1986) Vertical profile of lead isotope compositions in the Northeast Pacific. *Nature* **321,** 689–690.
Fuller C. and Hammond D. E. (1983) The fallout rate of Pb-210 on the Western coast of the United States. *Geophys. Res. Lett.* **10(12),** 1164–1167.
Goldstein S. J. and Jacobsen S. B. (1987) The Nd and Sr isotopic systematics of river-water dissolved material: Implications for the sources of Nd and Sr in seawater. *Chem. Geol.* **66,** 245–272.
Graustein W. C. and Turekian K. K. (1990) Radon fluxes from soils to the atmosphere measured by ^{210}Pb-^{226}Ra disequilibrium in soils. *Geophys. Res. Lett.* **17(6),** 841–844.
Grousset F. E., Biscaye P. E., Revel M., Petit J.-R., Pye K., Joussaume S., and Jouzel J. (1992) Antarctic (Dome C) ice-core dust at 18 k.y. B.P.: Isotopic constraints on origins. *Earth Planet. Sci. Lett.* **111,** 175–182.
Hamelin B., Grousset F. E., Biscaye P. E., and Zindler A. (1989) Lead isotopes in trade wind aerosols at Barbados: The influence of European emissions over the North Atlantic. *J. Geophys. Res.* **94(C11),**16243–16250.
Heinze C., Maier-Reimer E., and Winn K. (1991) Glacial pCO_2 reduction by the world ocean: Experiments with the Hamburg carbon cycle model. *Paleoceanography* **6,** 395–430.
Heinze C., Maier-Reimer E., Winguth A. M. E., and Archer D. (1999) A global oceanic sediment model for longterm climate studies. *Global Biogeochem. Cycles* **13(1),** 221–250.
Hemming S. R. and McClenan S. (2001) Pb isotope compositions of modern deep-sea turbidites. *Earth Planet. Sci. Lett.* **184,** 489–503.
Henderson G. M., Martel D. J., O'Nions R. K., and Shackleton N. J. (1994) Evolution of seawater ^{87}Sr/^{86}Sr over the last 400 ka: The absence of glacial/interglacial cycles. *Earth Planet. Sci. Lett.* **128,** 643–651.
Henderson G. M., Heinze C., Anderson R. F., and Winguth A. M. E. (1999) Global distribution of the ^{230}Th flux to ocean sediments constrained by GCM modeling. *Deep-Sea Res.* **46(11),** 1861–1893.
Igel H. and von Blanckenburg F. (1999) Lateral mixing and advection of reactive isotope tracers in ocean basins: Numerical modeling. *Geochem. Geophys. Geosyst.* **1,** GC000003.
Jones C. E., Halliday A. E., Rea D. K., and Owen R. M. (2000) Eolian inputs of lead to the North Pacific. *Geochim. Cosmochim. Acta* **64,** 1405–1416.
Ku T. L. and Lin M. C. (1976) ^{226}Ra distribution in the Antarctic ocean. *Earth Planet. Sci. Lett.* **32,** 236–248.
Ku T.-L. and Luo S. (1994) New appraisal of radium 226 as a large-scale oceanic mixing tracer. *J. Geophys. Res.* **99(C5),** 10255–10273.
Lee H. N. and Feichter J. (1995) An intercomparison of wet precipitation scavenging schemes and the emission rates of Rn-222 for the simulation of global transport and deposition of Pb-210. *J. Geophys. Res.* **100(D11),** 23253–23270.
Lin X., Zaucker F., Hsie E. Y., Trainer M., and McKeen S. A. (1996) Radon 222 simulations as a test of a three-dimensional regional transport model. *J. Geophys. Res.* **101(D22),**29165–29177.
Maier-Reimer E. (1993) Geochemical cycles in an ocean general circulation model. Preindustrial tracer distributions. *Global Biogeochem. Cycles* **7(3),** 645–677.
Maier-Reimer E., Mikolajewicz U., and Hasselmann K. (1993) Mean circulation of the Hamburg LSG OGCM and its sensitivity to the thermohaline surface forcing. *J. Phys. Oceanogr.* **23,** 731–757.
Maier-Reimer E. and Henderson G. (1998) ^{210}Pb in the ocean: A pilot tracer for modeling particle reactive elements. *Proc. Indian Acad. Sci. (Earth Planet. Sci.)* **107(4),** 351–357.
Maring H. B. and Duce R. A. (1987) The impact of atmospheric aerosols on trace metal chemistry in open ocean surface seawater, 1. *Aluminum Earth Planet. Sci. Lett.* **84,** 381–392.
Moore R. M. and Smith J. N. (1986) Disequilibrium between ^{226}Ra, ^{210}Pb and ^{210}Po in the Arctic Ocean and the implications for chemical modification of the Pacific water inflow. *Earth Planet. Sci. Lett.* **77,** 285–292.
Nozaki Y. and Tsunogai S. (1976) ^{226}Ra, ^{210}Pb and ^{210}Po disequilibria in the western North Pacific. *Earth Planet. Sci. Lett.* **32,** 313–321.

Nozaki Y., Thomson J., and Turekian K. K. (1976) The distribution of ^{210}Pb and ^{210}Po in the surface waters of the Pacific Ocean. *Earth Planet. Sci. Lett.* **32,** 304–3.

Nozaki Y., Turekian K. K., and Von Damm K. (1980) ^{210}Pb in GEOSECS water profiles from the North Pacific. *Earth Planet. Sci. Lett.* **49,** 393–400.

Nozaki Y., Tsubota H., Kasemsupaya V., Yashima M., and Ikuta N. (1991) Residence times of surface water and particle-reactive ^{210}Pb and ^{210}Po in the East China and Yellow Seas. *Geochim. Cosmochim. Acta* **55,** 1265–1272.

Nriagu J. (1979) Global inventory of natural and anthropogenic emissions of trace metals to the atmosphere. *Nature* **279,** 409–411.

O'Nions R. K., Carter S. R., Cohen R. S., Evensen N. M., and Hamilton P. J. (1978) Pb, Nd and Sr isotopes in oceanic ferromanganese deposits and ocean floor basalts. *Nature* **273,** 435–438.

O'Nions R. K., Frank M., von Blanckenburg F., and Ling H.-F. (1998) Secular variation of Nd and Pb isotopes in ferromangenese crusts from the Atlantic, Indian and Pacific oceans. *Earth Planet. Sci. Lett.* **155,** 15–28.

Ostlund H. G., Craig H., Broecker W. S., and Spencer D. (1987) *GEOSECS Atlantic, Pacific and Indian Ocean Expeditions*,Vol. 7, *Shorebased Data and Graphics*, U.S. Government.

Patterson C. C. and Settle D. M. (1987) Review of data on eolian fluxes of industrial and natural lead to the lands and seas in remote regions on a global scale. *Mar. Chem.* **22,** 163–177.

Reynolds P. H. and Dasch E. J. (1971) Lead isotopes in marine manganese nodules and the ore-lead growth curve. *J. Geophys. Res.* **76(21),** 5124–5129.

Settle D. M., Patterson C. C., Turekian K. K., and Cochran J. K. (1982) Lead precipitation fluxes at tropical oceanic sites determined from ^{210}Pb measurements. *J. Geophys. Res.* **87(C2),**1239–1245.

Shannon L. V., Cherry R. D., and Orren M. J. (1970) Polonium-210 and lead-210 in the marine environment. *Geochim. Cosmochim. Acta* **34,** 701–711.

Shen G. T. and Boyle E. A. (1987) Lead in corals: Reconstruction of historical industrial fluxes to the surface ocean. *Earth Planet. Sci. Lett.* **82,** 289–304.

Shen G. T. and Boyle E. A. (1988) Thermocline ventilation of anthropogenic lead in the western North Atlantic. *J. Geophys. Res.* **93(C12),**15715–15732.

Sherrell R. M. and Boyle E. A. (1992) Isotopic equilibration between dissolved and suspended particulate lead in the Atlantic ocean: Evidence from ^{210}Pb and stable Pb isotopes. *J. Geophys. Res.* **97(C7),**11257–11268.

Somayajulu B. L. K. and Craig H. (1976) Particulate and soluble ^{210}Pb activities in the deep sea. *Earth Planet. Sci. Lett.* **32,** 268–276.

Spencer D. W., Bacon M. P., and Brewer P. G. (1981) Models of the distribution of ^{210}Pb in a section across the North Equatorial Atlantic Ocean. *J. Mar. Res.* **39(1),** 119–137.

Thomson J. and Turekian K. K. (1976) ^{210}Po and ^{210}Pb distributions in ocean water profiles from the eastern south Pacific. *Earth Planet. Sci. Lett.* **32,** 297–303.

Thomson J., Colley S., Anderson R., Cook G. T., and MacKenzie A. B. (1993) ^{210}Pb in the sediments and water column of the Northeast Atlantic from 47 to 59°N along 20°W. *Earth Planet. Sci. Lett.* **115,** 75–87.

Turekian K. K. and Cochran J. K. (1981) ^{210}Pb in surface air at Enewetak and the Asian dust flux to the Pacific. *Nature* **292,** 522–524.

Turekian K. K., Benninger L. K., and Dion E. P. (1983) ^{7}Be and ^{210}Pb total deposition fluxes at New Haven, Connecticut, and at Bermuda. *J. Geophys. Res.* **88(C9),**5411–5415.

von Blanckenburg F., O'Nions R. K., and Hein J. R. (1996) Distribution and sources of pre-anthropogenic lead isotopes in deep ocean water from Fe-Mn crusts. *Geochim. Cosmochim. Acta* **60,** 4957–4964.

von Blanckenburg F. and Igel H. (1999) Lateral mixing and advection of reactive isotope tracers in ocean basins: Observations and mechanisms. *Earth Planet. Sci. Lett.* **169,** 113–128.

White W. M. and Dupre B. (1985) Isotope and trace element geochemistry of sediments from the Barbados Ridge—Demerara plain region, Atlantic Ocean. *Geochim. Cosmochim. Acta* **49,** 1875–1886.

Windom H. L., Smith R. G., and Maeda M. (1985) The geochemistry of lead in rivers, estuaries and the continental shelf of the southeastern United States. *Mar. Chem.* **17,** 43–56.

Windom H., Smith R., Rawlinson C., Hungspreugs M., Dharmvanij S., and Wattayakorn G. (1988) Trace metal transport in a tropical estuary. *Mar. Chem.* **24,** 293–305.

Winguth A. M. E., Archer D, Duplessy J.-C., Maier-Reimer E., and Mikolajewicz U. (1999) Sensitivity of paleonutrient tracer distributions and deep-sea circulation model to glacial boundary conditions. *Paleoceanography* **14,** 304–323.